Analysis of patient-specific surgical ventricular restoration: importance of an ellipsoidal left ventricular geometry for diastolic and systolic function

Lik Chuan Lee, Jonathan F. Wenk, Liang Zhong, Doron Klepach, Zhihong Zhang, Liang Ge, Mark B. Ratcliffe, Tarek I. Zohdi, Edward Hsu, Jose L. Navia, Ghassan S. Kassab and Julius M. Guccione

J Appl Physiol 115:136-144, 2013. First published 2 May 2013;
doi: 10.1152/japplphysiol.00662.2012

J Appl Physiol 115: 136–144, 2013.
First published May 2, 2013; doi:10.1152/japplphysiol.00662.2012.

Analysis of patient-specific surgical ventricular restoration: importance of an ellipsoidal left ventricular geometry for diastolic and systolic function

Lik Chuan Lee,[1,2] Jonathan F. Wenk,[3] Liang Zhong,[4] Doron Klepach,[1,2] Zhihong Zhang,[1] Liang Ge,[1,2] Mark B. Ratcliffe,[1,2] Tarek I. Zohdi,[5] Edward Hsu,[6] Jose L. Navia,[7] Ghassan S. Kassab,[8] and Julius M. Guccione[1,2]

[1]*Department of Surgery, University of California, San Francisco, California;* [2]*Department of Bioengineering, University of California, San Francisco, California;* [3]*Department of Mechanical Engineering and Surgery, University of Kentucky, Lexington, Kentucky;* [4]*Department of Cardiology, National Heart Centre Singapore, and Duke-NUS Graduate Medical School, Singapore;* [5]*Department of Mechanical Engineering, University of California, Berkeley, California;* [6]*Department of Bioengineering, The University of Utah, Salt Lake City, Utah;* [7]*Cleveland Clinic, Cleveland, Ohio; and* [8]*Department of Biomedical Engineering, Indiana University-Purdue University, Indianapolis, Indiana*

Submitted 1 June 2012; accepted in final form 10 April 2013

Lee LC, Wenk JF, Zhong L, Klepach D, Zhang Z, Ge L, Ratcliffe MB, Zohdi TI, Hsu E, Navia JL, Kassab GS, Guccione JM. Analysis of patient-specific surgical ventricular restoration: importance of an ellipsoidal left ventricular geometry for diastolic and systolic function. *J Appl Physiol* 115: 136–144, 2013. First published May 2, 2013; doi:10.1152/japplphysiol.00662.2012.—Surgical ventricular restoration (SVR) is a procedure designed to treat heart failure by surgically excluding infarcted tissues from the dilated failing left ventricle. To elucidate and predict the effects of geometrical changes from SVR on cardiac function, we created patient-specific mathematical (finite-element) left ventricular models before and after surgery using untagged magnetic resonance images. Our results predict that the postsurgical improvement in systolic function was compromised by a decrease in diastolic distensibility in patients. These two conflicting effects typically manifested as a more depressed Starling relationship (stroke volume vs. end-diastolic pressure) after surgery. By simulating a restoration of the left ventricle back to its measured baseline sphericity, we show that both diastolic and systolic function improved. This result confirms that the increase in left ventricular sphericity commonly observed after SVR (endoventricular circular patch plasty) has a negative impact and contributes partly to the depressed Starling relationship. On the other hand, peak myofiber stress was reduced substantially (by 50%) after SVR, and the resultant left ventricular myofiber stress distribution became more uniform. This significant reduction in myofiber stress after SVR may help reduce adverse remodeling of the left ventricle. These results are consistent with the speculation proposed in the Surgical Treatment for Ischemic Heart Failure trial (20) for the neutral outcome, that "the lack of benefit seen with surgical ventricular reconstruction is that benefits anticipated from surgical reduction of left ventricular volume (reduced wall stress and improvement in systolic function) are counter-balanced by a reduction in diastolic distensibility."

myocardial infarction; surgical ventricular restoration; finite-element modeling; coronary artery bypass grafting

SURGICAL VENTRICULAR RESTORATION (SVR) is a procedure designed to treat heart failure by surgically excluding infarcted tissues from the dilated failing left ventricle (LV). The aim of this treatment is to neutralize the negative physiological effects of dysfunctional regions in the LV wall. The Surgical Treatment for Ischemic Heart Failure (STICH) trial was conducted to assess the effectiveness of SVR (35). One of the two components of the trial was to determine whether adding SVR to coronary artery bypass grafting (CABG) would decrease the rate of death or hospitalization for cardiac causes more than CABG alone. The clinical findings led the authors to conclude that adding SVR to CABG reduces the LV volume compared with CABG alone, but this reduction is not associated with a greater improvement in symptoms, exercise tolerance, or a reduction in the rate of death or hospitalization for cardiac causes. One speculation for these findings was that the benefits anticipated from the surgical reduction of LV volume were counterbalanced by a reduction in diastolic distensibility (21).

Although the STICH trial concluded that SVR, when performed with CABG, adds no benefits to the patient, this conclusion remains controversial (7, 8, 26). Clinical studies have shown that SVR did benefit patients who had myocardial infarction (3, 4, 8, 19, 24, 28), and both the European Society of Cardiology and European Association for Cardio-Thoracic Surgery recommend SVR if LV volume is measured, scar is identified, and surgery is performed in centers with a high level of surgical expertise (37). Conversely, clinical studies have also shown that stroke volume (SV) decreased after SVR (13, 22, 34, 39), and the decrease in size of the LV after SVR can be accompanied by an increase in LV sphericity (12, 23, 39). This postsurgical increase in LV sphericity was believed to impair diastolic function (27). On the other hand, the supposedly lower ventricular wall stress (based on Laplace's law) resulting from a reduction in LV size after SVR should, in principle, benefit patients by reducing myocardial oxygen demand (29). These conflicting effects of SVR contribute, in part, to the gap in our understanding as to why patients who underwent SVR did not always receive the benefits from the supposedly lower wall stress. Bridging this gap requires accurate quantification of the local myofiber stress, which, at present, can be determined only through patient-specific mathematical modeling (38).

Patient-specific mathematical modeling of the effects of SVR is largely lacking and is, at best, overly simplified. Many mathematical analyses of SVR have been conducted based on animal LV models. For example, a mathematical model of the sheep LV by Dang et al. (10) was used to study the effects of SVR alone (without CABG) on diastolic distensibility, end-systolic (ES) elastance, the Starling relationship [SV vs. end-

Address for reprint requests and other correspondence: J. M. Guccione, UCSF/VA Medical Center (112D), 4150 Clement St., San Francisco, CA 94121 (e-mail: julius.guccione@ucsfmedctr.org).

diastolic (ED) pressure], and regional myofiber stress distribution. Their results suggest that, compared with the remote region, SVR reduces myofiber stress in the akinetic infarct and infarct border zone. They also found that the Starling relationship was depressed after SVR. However, this result is based on a sheep LV and did not address the increase in sphericity of the postsurgical LV commonly found in patients. On the other hand, a recent analysis of the patient-specific effects of SVR found it reduced the LV bulk wall stress and improved the LV systolic function (40). That analysis was based on a local balance of forces, however, and cannot account for myofiber orientation or predict myofiber stress distribution within the LV (38).

To elucidate the functional effects resulting from the geometrical change found in the LV after SVR, we performed the first mathematical analysis on the effects of SVR using patient-specific finite-element (FE) LV models. These models were created using untagged magnetic resonance (MR) images from the same set of patient data described in Zhong et al. (39).

MATERIAL AND METHODS

Acquisition of MR images. The method used for MR imaging (MRI) is detailed in Zhong et al. (40). All procedures in patients were approved by our institutional review board, and patient consents were obtained. The MR images were de-identified. Images were obtained 1–2 wk before surgery and 1–2 wk after surgery with a 1.5-T MRI scanner (Siemens Somatom, Erlangen, Germany). These images were segmented interactively by outlining the LV endocardial and epicardial borders (excluding papillary muscles and trabeculation) using CMR tools. Then the set of LV contour points derived from the segmentation process was triangulated using Rapidform (INUS Technology) to reconstruct the three-dimensional (3D) LV epicardial and endocardial surfaces. ED and ES cardiac phases were determined by visualizing the mitral valve and the aortic valve closure.

FE modeling. We used the FE method to analyze the effects of surgery (CABG + SVR) in 12 patients (randomly selected from a cohort of 40 patients). In each patient, the SVR procedure was performed using the endoventricular circular patch plasty technique. Three of these 12 patients had concomitant mitral regurgitation and underwent mitral valve repair (MVR) surgery by means of restrictive mitral annuloplasty. A multivariable general linear model analysis was performed on this patient cohort and did not detect any differences between patients who received MVR surgery and patients who did not receive MVR (39). FE models of the LV were created by projecting a mesh between the 3D endocardial and the 3D epicardial surface reconstructed from the acquired MR images (32) at early diastole (Truegrid, XYZ Scientific Applications, Livermore, CA). The mesh in each LV model consisted of between 2,000 and 4,000 trilinear eight-noded brick elements.

In the presurgery models, two distinct material regions were defined: the transmural infarct region and the remote region. The infarct region was defined as the region without any relative wall motion; i.e., akinesia. The remote-infarct boundary was identified by overlapping the ED and the ES endocardial surface. Then this boundary was projected transmurally onto the epicardial surface. In the postsurgery models, the entire LV was assumed to be composed of a single material, as there were no significant overlapping regions. Residual stress was not included in the postsurgery LV models, because the effects were found to be negligible in a previous study (16). Rigid body motion of the LV was suppressed by constraining the base from moving in the longitudinal direction and by constraining the epicardial-basal edge from moving in all directions.

Myofiber angle distribution was assumed to vary transmurally from epicardium to endocardium via a linear transition from -60 to $+60°$ relative to the circumferential direction in all models (16, 30). Also, we have recently obtained unpublished ex vivo diffusion tensor MRI fiber angle measurements from five explanted human hearts with ischemic heart failure. The myofiber angle was found to vary transmurally from $-42.4°$ (epicardium) to $35.7°$ (endocardium), on average. To test whether the conclusions of our analysis would be impacted if these new fiber angle data were used, we repeated the analysis on one LV model using these new fiber data.

Because pressure was not measured in the LV, the ES pressure (ESP) was assumed to match the measured systolic blood pressure (SBP) of individual patients. The average SBP of the patients was 121 mmHg presurgery and 117 mmHg postsurgery. ED pressure (EDP) was assumed to be 12 mmHg presurgery and postsurgery. The pressure was applied to the LV endocardial surface. To assess the sensitivity of the pressure-volume and Starling relationship to EDP and ESP, we repeated the analysis with EDP at 4 and 20 mmHg and ESP at 90 and 110% of the SBP. The sensitivity of the ES myofiber stress to ESP was also assessed for each case. We note that the estimation of ESP $= 0.9 \times$ SBP, as was used in many studies (e.g., in Ref. 5), falls within the range of ESP used in our sensitivity analysis. Although the sensitivity analysis did not account for inter-individual differences in the LV pressure (especially in EDP), it did confirm that the overall conclusions of this study are not sensitive to the LV pressure assumptions.

Passive and active constitutive laws previously described by Guccione et al. (17, 18) were used in this study (see the Appendix). The constitutive laws were implemented with a user-defined material subroutine in LS-DYNA (Livermore Software Technology, Livermore, CA). Passive stiffness of myocardial tissue was characterized by the material parameter C in the constitutive law. To obtain C in each of the model, we adjusted the C values so that the predicted LV cavity volume of the FE model matched the measured ED volume (EDV). In the presurgery models, C at infarct (C_I) was set to be 10 times stiffer than that in the remote region (C_R) (36). Myocardial tissue contractility in the active constitutive law was characterized by the material parameter T_{max}, which is the strength of contraction at the longest sarcomere length in the tissue. In the postsurgery FE models, T_{max} was adjusted so that the predicted LV cavity volume matched the measured ES volume (ESV). In the presurgery FE models, T_{max} at the infarct and at the remote region were optimized so that *1*) the radial strain was nominally zero at the infarct because changes in wall thickness are minimal in akinesia, and *2*) the predicted LV cavity volume subjected to ESP was within $\pm 1\%$ of the measured ESV. The optimization was implemented using LS-OPT (Livermore Software Technology, Livermore, CA). The approach of determining active material parameters in the presurgery models was adopted from Dang et al. (11), who have used FE models extrapolated from two-dimensional echocardiography to examine akinetic infarcts. Although our models did not physically include any postsurgical implants (e.g., rigid rings, patches), the mechanical effects of these implants were, nevertheless, reflected in the material parameters C and T_{max} as they were calculated based on the MRI-measured LV volumes and LV pressures that are within a physiological range.

Two postsurgery FE models were used to perform a study on the effects of LV sphericity, which was quantified by the short-to-long-axis ratio or sphericity index (SI). The long-axis dimension was defined to be the apex-to-base distance, and the short-axis dimension was defined to be the maximum epicardial diameter measured at the mid-LV; i.e., half-way between apex and base. A large value of SI indicates a more spherical LV, whereas a small value of SI indicates a more ellipsoidal LV. To simulate a change in SI, a downward force was applied at the apical region to elongate the LV, and a negative pressure was concurrently applied at the midbasal endocardial wall to ensure that the LV cavity volume remained constant. Then the resultant LV geometry was used as the initial "stress-free" configuration to which the same fiber angle distribution was assigned. Because the myocardial material is incompressible, the LV wall mass

remained constant after the LV shape was modified. The downward force was not present in subsequent analyses performed on the resultant LV. This force was used purely for modifying the geometry of the LV. The corresponding postsurgery material parameters C and T_{max} were used in the elongated LV models.

Pressure-volume and Starling relationships. Global LV performance was quantified using the pressure-volume relationship at ED and ES, as well as by the Starling relationship. To obtain the EDP-EDV relationship (EDPVR), the FE models were used to predict the LV EDV at different EDP, ranging between 0 to 25 mmHg. Then the resulting pressure-volume relationship was fitted using an exponential function.

$$\mathrm{EDP} = A\left[e^{K_{ED}\cdot(\mathrm{EDV}-\mathrm{V}_{0,ED})} - 1\right] \quad (1)$$

In *Eq. 1*, A, $V_{0,ED}$, and K_{ED} are the fitting parameters. The parameter $V_{0,ED}$ is the LV volume at zero pressure, whereas the parameters K_{ED} and A affect the LV compliance during filling. Diastolic function was quantified using the linear slope of EDPVR at 12 mmHg (E_{ED}). An improvement in diastolic function was characterized by a decrease in E_{ED}.

The ESP-EDV relationship (ESPVR) was obtained from the FE models by simulating the LV at different ESP, ranging from 0 to 140 mmHg. The computed LV ESVs were fitted to the corresponding applied ESPs using a linear function (2, 31), as given in the next equation:

$$\mathrm{ESP} = \mathrm{E}_{ES}\left(\mathrm{ESV} - \mathrm{V}_{0,ES}\right) \quad (2)$$

An improvement in systolic function is characterized by an increase in the ES elastance E_{ES}, i.e., the gradient of the linear fit, as well as by a decrease in the volume intersection $V_{0,ES}$ of the ESPVR. The simultaneous improvement of the diastolic and systolic function translates to an improvement in SV and the Starling relationship.

To calculate the Starling relationship, we followed the approach used in Dang et al. (10). The arterial elastance was calculated (for each case) from the measured SV, the measured EDV, the fitted E_{ES}, and the volume-intersect $V_{0,ES}$ of the ESPVR using *Eq. 3* in Dang et al. (10). Then the Starling relationship (SV-EDP) was obtained using that same equation by substituting for these values as well as for the computed EDPVR. We note that SV was not compensated in the three patients who had concomitant mitral regurgitation and underwent MVR surgery. In the study on the effects of sphericity, the arterial elastance was kept constant in each of the two groups. We have chosen here to use SV to quantify the LV performance instead of ejection fraction because ejection fraction is not an independent measure of LV performance after SVR (i.e., it is also sensitive to the decrease in EDV after surgery).

RESULTS

Unless otherwise indicated, all results are reported as means ± SD. Individual results from each patient are shown in the supplemental materials. (The online version of this article contains supplemental data.)

Reconstructed LV geometries and hemodynamics measurements. Figure 1*A* shows a representation of the presurgery and postsurgery FE LV model from 12 patients. The remote region is illustrated by the lighter region, and, in the presurgery models, the darker region illustrates the infarct. On average, measured EDV decreased by 92.7 ± 31.0 ml (from 269.6 ± 63.5 to 176.9 ± 58.0 ml), and measured ESV decreased by 78.7 ± 30.1 ml (from 210.4 ± 62.5 to 131.7 ± 63.2 ml) after surgery. The measured heart rate of these patients increased by 6.8 ± 9.5 beats/min after surgery (from 73.0 ± 8.4 to 79.8 ± 8.4 beats/min), and the corresponding cardiac output decreased by 0.6 ± 1.5 l/min (from 4.3 ± 1.2 and 3.6 ± 1.5 l/min) after surgery. Measured systemic vascular resistance index increased by 620 ± 1,890 dyn·s·cm^{-5}·m^{-2} (from 2,670 ± 660 to 3,290 ± 1,820 dyn·s·cm^{-5}·m^{-2}) after surgery. We also found that the LV became invariably more spherical after surgery, as illustrated in Fig. 1*B*. On average, SI increased by 30%, from 0.72 ± 0.07 to 0.98 ± 0.11 after surgery.

Predicted global LV performance. Figure 2 shows a representation of the effects of surgery on the ESPVR and EDPVR found in a typical patient. The bounds of the pressure-volume relationship from the sensitivity analysis are also displayed in the figure. We found that ESPVR consistently shifted to the left and became steeper after surgery. On average, the decrease in volume-intersect $V_{0,ES}$ after surgery was 64.1 ± 26.2 ml (from 159.2 ± 51.0 to 95.1 ± 51.3 ml), and the ES elastance E_{ES} increased by more than 1.5 times (from 2.40 ± 0.81 to 3.93 ± 2.20 mmHg/ml). Global systolic function, therefore, improved after surgery. This result was also insensitive to the choice of ESP. For the range of ESP at 90–110% of the SBP, the average

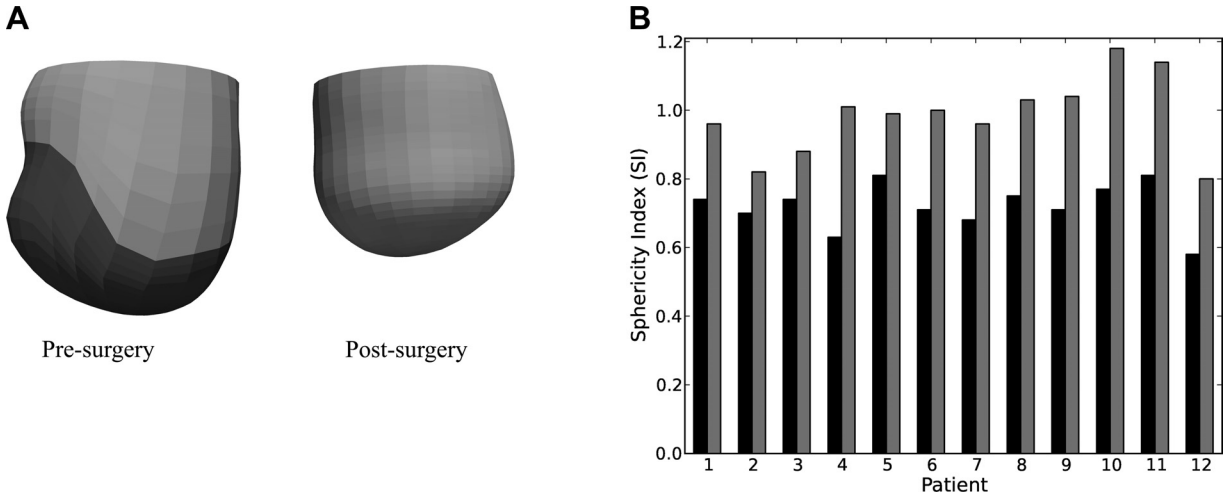

Fig. 1. *A*: representative finite-element left ventricular (LV) model taken from *patient 1* pre- (*left*) and postsurgery (*right*). In the presurgery models, dark and light regions define the infarct and the remote region, respectively. *B*: sphericity index (SI) of the 12 patients before surgery (solid bars) and after surgery (shaded bars).

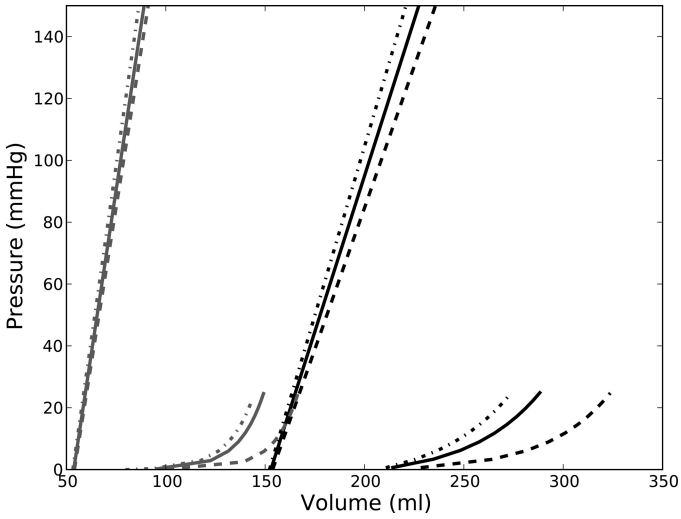

Fig. 2. End-diastolic pressure (EDP)-volume relationship (EDPVR) and end-systolic pressure (ESP)-volume relationship (ESPVR) after surgery (*patient 1*). Solid line, presurgery; shaded line, postsurgery. Line type indicates the pressure-volume relationships resulting from the different prescribed values of ESP and EDP: dashed line: EDP = 4 mmHg and ESP = 90% of systolic blood pressure (SBP); solid line = 12 mmHg and ESP = SBP; dot-dash line: EDP = 20 mmHg and ESP = 110% of SBP.

values of $V_{0,ES}$ and E_{ES} before surgery fell within 158.4–160.0 ml and 2.22–2.57 mmHg/ml, respectively. After surgery, the average values of $V_{0,ES}$ and E_{ES} for this range of ESP fell within 94.7–95.7 ml and 3.55–4.25 mmHg/ml, respectively.

Although global systolic function improved, global diastolic function worsened after surgery, and the LV became less compliant during filling. Specifically, ED elastance E_{ED} increased from 0.48 ± 0.15 to 0.82 ± 0.46 mmHg/ml after surgery. For the range of EDP of 4–20 mmHg, the average value of E_{ED} before surgery fell within 0.45–0.52 mmHg/ml, respectively. After surgery, the average values of E_{ED} for this range of EDP fell within 0.78–0.92 mmHg/ml, respectively. Therefore, the decrease in global diastolic function predicted by our mathematical models was also insensitive to the choice of EDP.

These counteracting effects found in the ESPVR and EDPVR typically translated to a more depressed Starling relationship. The predicted Starling relationship remained unchanged in three patients (Fig. 3*A*), worsened in eight patients (Fig. 3*B*), and improved only in one (Fig. 3*C*). Overall, SV decreased from 59.1 ± 18.5 to 45.1 ± 19.1 ml, an average drop of 14 ml. Hence, the improvement gained in the systolic function after surgery was negated by a worsening diastolic function in most cases.

Predicted myofiber stress distribution. Figure 4*A* shows the effect of surgery on the LV regional myofiber stress at end systole in a representative patient. Before surgery, myofiber stress was highly inhomogeneous in the LV and was significantly elevated at the thin apical region where the infarct resides. After surgery, the decrease in LV size was accompanied by an increase in LV wall thickness, which led to a significant reduction in the peak myofiber stress. As a result, the myofiber stress distribution became more homogeneous after surgery. Figure 4*B* shows the peak myofiber stress in the LV before and after surgery in all 12 patients. Peak myofiber stress after SVR was substantially reduced in all patients, regardless of whether this comparison was made with the peak myofiber stress found in the remote region of the presurgery LV or in the entire presurgery LV. On average, peak myofiber stress decreased by 50% (from 141.2 ± 45.1 to 70.3 ± 15.0 kPa) compared with the remote region of the presurgery LV.

Predicted effects of LV sphericity. Figure 5 shows the effects of sphericity on the postsurgical LV model from *patient 1*. Similar effects were also found in *patient 2* (not shown). Figure 5*A* shows the geometry of the postsurgical LV as it was "virtually elongated" (from the original postsurgery SI of 0.96 to an SI of 0.67) using the method described in the last paragraph of *FE modeling*. The LV cavity volume and the LV wall mass remained constant during this virtual "elongation" process. Figure 5*B* shows the ESPVR and EDPVR with SI as a parameter. As SI decreased, or equivalently, as the LV became more elongated, it became more compliant, and diastolic function improved as a result. For *patient 1*, E_{ED} decreased moderately by ~6% (from 0.96 to 0.90 mmHg/ml) with a 30% decrease in SI. Roughly the same percentage of decrease in E_{ED} was also seen in *patient 2* when SI decreased from 0.82 to 0.63. Similar to the effects of SI on diastolic function, systolic function also improved slightly as SI decreased. As SI decreased in *patient 1*, E_{ES} increased slightly from 4.40 to 4.46 mmHg/ml and $V_{0,ES}$ decreased from 53.1 to 50.6 ml. The same percentage of improvement in systolic function was also found in *patient 2* when SI decreased. The concurrent improvements in systolic and diastolic function were translated into an improvement in the Starling relationship (Fig. 5*C*). For an EDP between 4 to 20 mmHg, SV increased by ~3.5 ml in both patients after a 30% reduction in SI. The diastolic and systolic function and the Starling relationship did not improve after further reduction of SI.

All of the above-mentioned results were found to be relatively insensitive to a change in fiber angle distribution based on the repeated analysis (on one patient) using the recently acquired transmural linear variation of fiber angle from −42.4° (epicardium) to 35.7° (endocardium).

DISCUSSION

Effects on SV, systolic and diastolic function. The improvement in systolic function after SVR was compromised by a concurrent decrease in the LV diastolic distensibility. This conclusion is broadly consistent with the speculation offered from the STICH trial (21) and the findings from clinical studies by Tulner et al. (34) and Brinke et al. (6), who observed similar effects of the surgery on EDPVR when invasive pressure-volume measurements were used directly after cardiopulmonary bypass (34) and 6 mo after surgery (6). Specifically, K_{ED} was found to increase from 0.021 ± 0.009 to 0.037 ± 0.021 ml^{-1} after surgery in Tulner et al., and from 0.012 ± 0.003 to 0.023 ± 0.007 ml^{-1} after surgery in Brinke et al. In the clinical study by Brinke et al., ED elastance E_{ED} (taken at 18 mmHg) was also found to have increased from 0.15 ± 0.08 to 0.24 ± 0.10 mmHg/ml after surgery. Although our prediction of E_{ED} (0.48 ± 0.15 and 0.82 ± 0.46 mmHg/ml at pre- and postsurgery, respectively) is larger than the measurements by Brinke et al., the percent increase is comparable. In terms of ESPVR, Tulner et al. found that E_{ES} improved from 1.12 ± 0.63 to 1.57 ± 0.55 mmHg/ml, whereas Brinke et al. reported no significant change in E_{ES} (1.2 ± 0.6 mmHg/ml) at 6 mo after surgery.

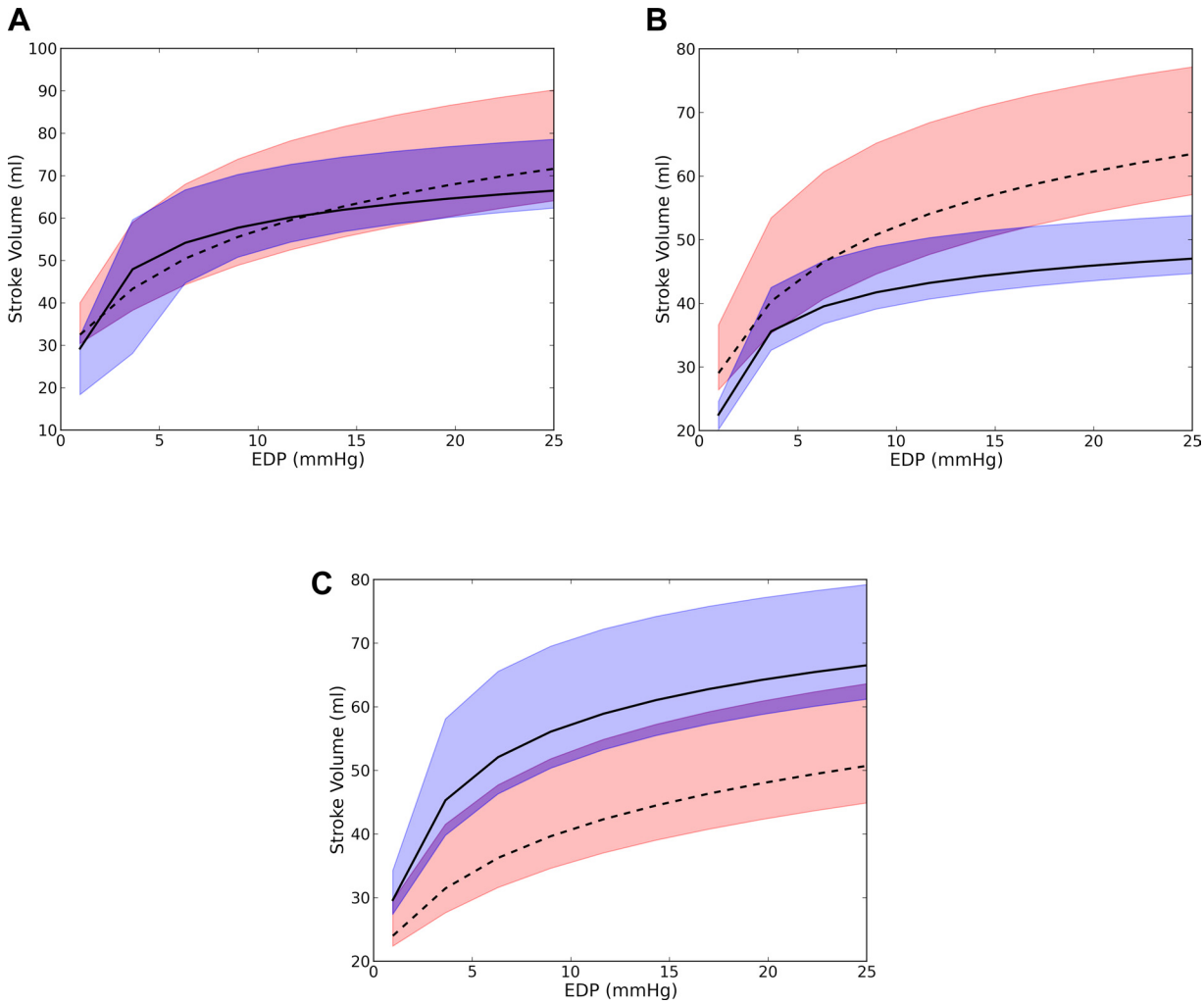

Fig. 3. Representative Starling relationship from three patients showing no significant changes (*patient 1*; *A*), worsening (*patient 2*; *B*), and improvement after surgery (*patient 4*; *C*). Dashed line, presurgery; solid line, postsurgery. Bounds of the predicted Starling relationship are shown as the red region for presurgery and as the blue region for postsurgery. These bounds were calculated from the EDPVR and ESPVR obtained by assuming an EDP of 4 and 20 mmHg and an ESP of 90 and 110% of the systolic blood pressure.

Although these values were also smaller than our prediction (2.40 ± 0.81 and 3.93 ± 2.20 mmHg/ml before and after surgery, respectively), the percent improvement predicted by our mathematical models is comparable to that reported by Tulner et al.

As a result of the counteracting effects of surgery on ESPVR and EDPVR, our results show that the Starling relationship (or SV) was usually more depressed after surgery. This result is consistent with clinical findings (13, 22, 34, 39). The average decrease in SV found from these studies was ~7.5 ml (compared with a decrease of 14 ml found here). In the clinical study by Brinke et al. (6), SV improved from 60 ± 17 to 68 ± 13 ml 6 mo after surgery.

Effects of a more ellipsoidal LV. Our results show that the decrease in SV was also accompanied by an increase in SI after surgery. This finding is generally consistent with clinical findings, which show a decrease in SV (13, 22, 34, 39) and an increase in sphericity (12, 40) after SVR using endoventricular circular patch plasty. In contrast to what occurs after endoventricular circular patch plasty, the postsurgical LV was reported to have become more ellipsoidal when SVR was performed using septal anterior ventricular exclusion or Pacopexy technique (20). The values of SI reported here are larger than the values reported in Zhong et al. (40). This difference is because the short-axis dimension was taken to be the widest LV minor axis at the endocardium based on a four-chamber cine MRI view of the heart (40), whereas here, we have taken that dimension to be the maximum diameter of the MRI-reconstructed epicardial surface at the midventricle. Our prediction that a decrease in SI can improve the diastolic and systolic function is also consistent with the theoretical studies by Choi et al. (9) and Geerts et al. (14). In these studies, an idealized prolate LV was used to show that the LV became more compliant during filling as it became more ellipsoidal (9), and the LV pump function was reduced in a spherical LV compared with an ellipsoidal LV (14). Given that the LV EDVs were smaller (~80 ml) in these studies than those found here (EDV = 176.9 ± 58 ml), the effects of sphericity appear to be size independent, at least within the range of EDV mentioned here.

Our results show a decrease in SI by ~30% leads to an improvement in the Starling relationship of an ~3.5 ml increase in SV. This result suggests that the postsurgical increase

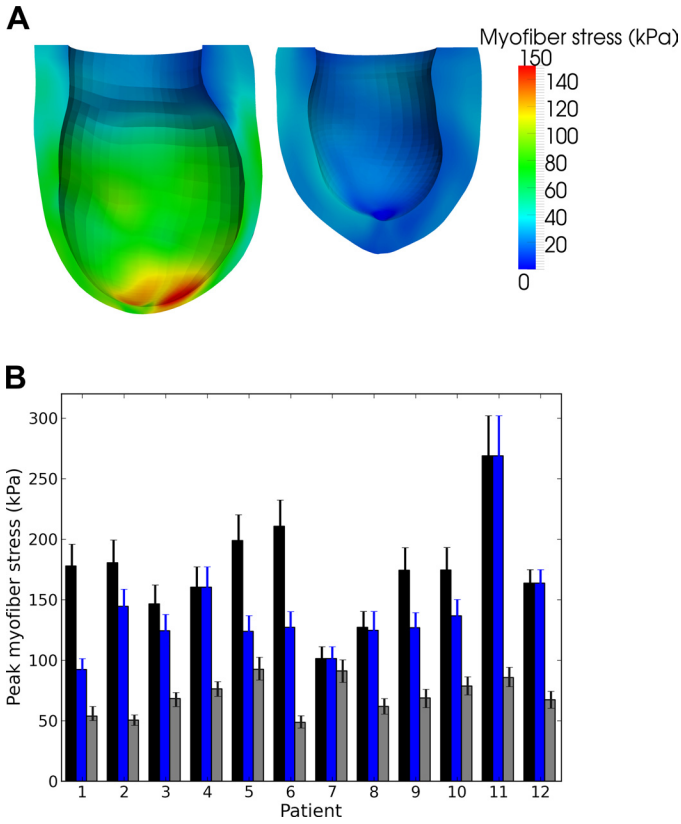

Fig. 4. *A*: representative end-systolic myofiber stress distribution taken from *patient 1*. *Left*: predicted regional myofiber stress in the presurgery LV. *Right*: stress in the more spherical postsurgery LV. *B*: peak end-systolic myofiber stress of the 12 patients before and after surgery. Black, blue, and gray bars indicate peak stress in the entire presurgery LV, in the presurgery LV's remote region, and in the entire postsurgery LV, respectively. Error bars show the bounds of the peak myofiber stress when ESP was varied between 90 and 110% of the SBP.

in SI contributes in part to the decrease in SV found after surgery. By restoring the LV SI back to its baseline value (~30% lower than in postsurgery SI), we showed that the decrease in SV associated with an increase in sphericity cannot fully account for the 14-ml postsurgical drop in SV. Therefore, it is likely that there are other mechanisms contributing to the decrease in SV other than the increased sphericity found after surgery.

Effects on myofiber stresses. Our results show that the peak end-systolic myofiber stress decreased significantly after surgery, in contrast to the compromised Starling relationship. Although the bulk wall stress can be predicted using Laplace's law, prediction of the myofiber stress and its distribution within the LV requires mathematical modeling (38). These results are, therefore, more accurate in predicting LV remodeling (1, 15, 33) and regional oxygen consumption (29). Our results confirm that SVR can reduce peak myofiber stress (by 50% on average), which can substantially reduce LV myocardial oxygen consumption (29). On the other hand, myofiber stress distribution may also become more homogeneous as a result of a more uniform ventricular wall thickness after surgery (Fig. 4*A*, *right*). Given that LV remodeling is widely believed to be initiated by an increase in both magnitude and inhomogeneity of myofiber stress (1, 15, 33), the more homogeneous myofiber stress distribution found after surgery suggests that SVR + CABG may attenuate further adverse remodeling of the LV. Whether SVR can successfully restore myofiber stress level and distribution to those found in the normal human LV and help to prevent further adverse LV remodeling will require knowledge of the myofiber stress distribution in the normal human LV.

Limitations. The limitations to our study are primarily due to the lack of acquired data. First, because MR images with delayed gadolinium enhancement were not available, infarcted regions in the LV were determined based on LV wall motion and were assumed to be transmural. As a result, other possible infarcted regions that are less severe, particularly regions exhibiting hypokinesia, may have been omitted in our mathematical LV models.

Second, we were forced to assume physiologically reasonable values of 12 mmHg as EDP for all patients and the measured SBP as ESP for individual patients, because patient-specific LV pressure data, which requires invasive measurements using micromanometer-tipped catheter, was not available. LV pressure, of course, tends to vary between patients. To overcome this limitation, we conducted sensitivity analysis to test whether our conclusions are affected by a variability in LV pressure. We have found that the conclusions are insensitive to a variation in LV pressure.

Conclusion. In this first FE analysis of the effects of CABG + SVR based on patient-specific MR images, we have quantified the global and regional functional effects resulting from geometrical changes of the LV due to surgery. The three main conclusions from our computational analysis are as follows. First, LV systolic function improved, whereas LV diastolic function worsened after SVR + CABG surgery. These conflicting effects resulted in a more depressed Starling relationship after surgery. Second, postsurgical increase in LV sphericity caused the SV to decrease, even though this decrease is insufficient to compensate for the drop in SV found after surgery. Third, the peak myofiber stress decreased substantially (50%), and the myofiber stress distribution became more uniform in the LV after SVR + CABG surgery. These findings are consistent with the speculation proposed in the STICH trial (20) for the neutral outcome, that "the lack of benefit seen with surgical ventricular reconstruction is that benefits anticipated from surgical reduction of LV volume (reduced wall stress and improvement in systolic function) are counter-balanced by a reduction in diastolic distensibility." Since the results we presented are based on LV models reconstructed from patients at only one clinical center (Cleveland Clinic) who underwent a specific type of SVR (endoventricular circular patch plasty), they may not include the effects found when SVR is performed in other centers or when the surgery is performed using other variants of SVR e.g., the Pacopexy technique (20), which may confer other benefits, as described by Buckberg et al. (7). Since the outcome of SVR is still largely controversial, with both the European Society of Cardiology and European Association for Cardio-Thoracic Surgery recommending SVR (37), despite the negative outcome of Hypothesis 2 of the STICH trial (21), more models of other SVR variants using patient data from other clinical centers are needed to assess patient-specific efficacy of SVR.

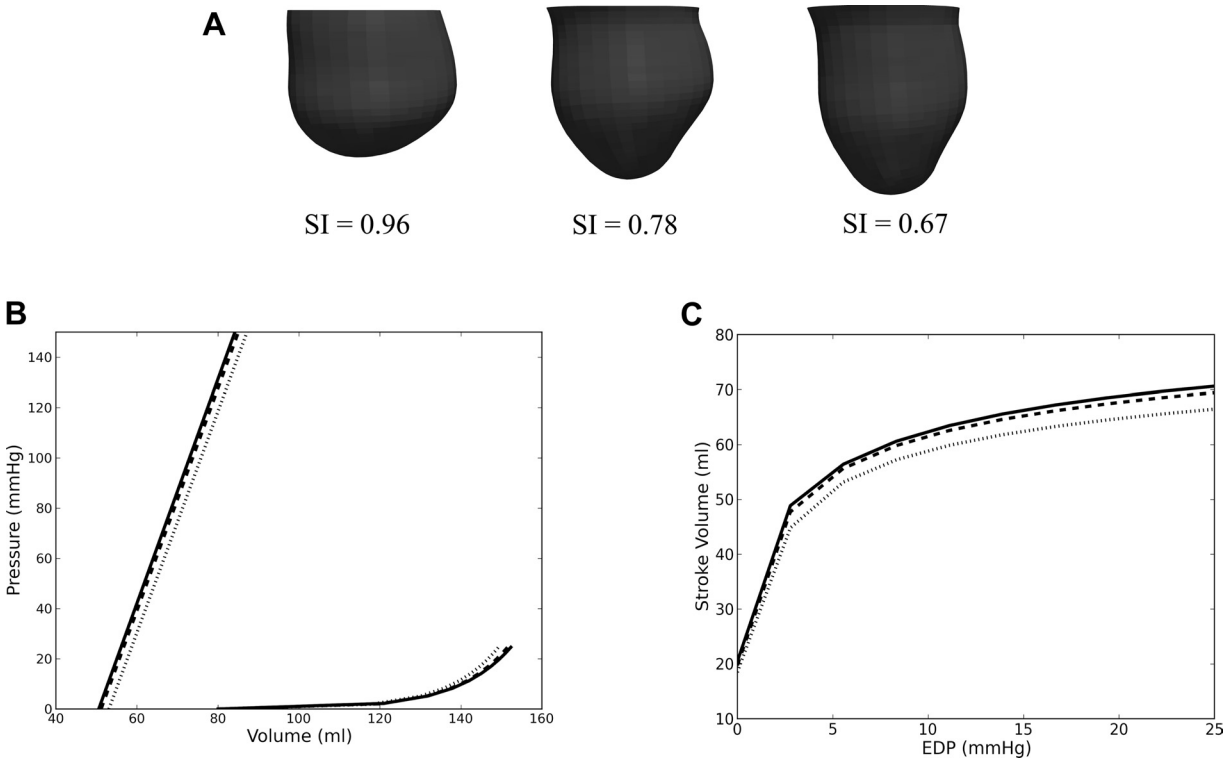

Fig. 5. *A*: LV with decreasing SI from *left* to *right*. The original LV of *patient 1* after surgery is shown on the *left*, and the "virtually elongated" LVs are on the *center* and *right*. *B*: effects of LV SI on EDPVR and ESPVR. *C*: the effects of LV SI on the Starling relationship. Dotted line, SI = 0.96; dashed line, SI = 0.78; and solid line, SI = 0.67.

APPENDIX: CONSTITUTIVE LAW OF THE MYOCARDIAL TISSUE

Nearly incompressible, transversely isotropic, hyperelastic constitutive laws for passive (18) and active myocardium (17) were used to model diastolic filling and active contraction. Passive material properties were represented by the strain energy function W:

$$W = \frac{C}{2}\left\{\exp\left[b_f \mathrm{E}_{11}^2 + b_t\left(\mathrm{E}_{22}^2 + \mathrm{E}_{33}^2 + \mathrm{E}_{23}^2 + \mathrm{E}_{32}^2\right) + b_{fs}\left(\mathrm{E}_{12}^2 + \mathrm{E}_{21}^2 + \mathrm{E}_{13}^2 + \mathrm{E}_{31}^2\right)\right] - 1\right\} \quad (A1)$$

where E_{11} is fiber strain, E_{22} is cross-fiber strain, E_{33} is radial strain, E_{23} is shear strain in the transverse plane, and E_{12} and E_{13} are shear strain in the fiber-cross fiber and fiber-radial planes, respectively. Values for the material constants b_f, b_t, and b_{fs} were obtained from large-animal studies and have values of 49.25, 19.25, and 17.44, respectively (32). The material constant C was adjusted until the LV EDVs matched the experimentally measured values, as described in the main text.

Active contraction was modeled by defining the total stress as the sum of the passive stress derived from the strain energy function W and an active fiber directional component, $\mathbf{T}_0$, which is a function of time, t, peak intracellular calcium concentration, Ca_0, sarcomere length, l, and maximum isometric tension achieved at the longest sarcomere length, $T_{\max}$ (17), i.e.

$$\mathbf{S} = pJ\mathbf{C}^{-1} + 2J^{-2/3}\mathrm{Dev}\left(\frac{\partial \widetilde{W}}{\partial \widetilde{C}}\right) + \mathbf{T}_0\left(t, \mathrm{Ca}_0, l; T_{\max}\right) \quad (A2)$$

In *Eq. A2*, $\mathbf{S}$ is the second Piola-Kirchoff stress tensor, p is the hydrostatic pressure introduced as the Lagrange multiplier needed to ensure incompressibility, J is the Jacobian of the deformation gradient tensor, $\mathbf{C}$ is the right Cauchy-Green deformation tensor, $\widetilde{\mathbf{C}}$ is the deviatoric decomposition of $\mathbf{C}$ (i.e., $\mathbf{C} = J^{2/3}\widetilde{\mathbf{C}}$), $\widetilde{W}$ is the deviatoric contribution of the strain energy function W given in *Eq. A1*, and Dev is the deviatoric projection operator defined as

$$\mathrm{DEV}(\bullet) = (\bullet) - \frac{1}{3}([\bullet] : \mathbf{C})\mathbf{C}^{-1} \quad (A3)$$

Assumption of near incompressibility of the myocardium also requires the decoupling of the strain energy function W into its dilational U and deviatoric components $\widetilde{W}$, i.e.

$$W = U(J) + \widetilde{W}\left(\widetilde{\mathbf{C}}\right) \quad (A4)$$

The active fiber-directed stress component is defined by a time-varying elastance model, which at end systole, is reduced to

$$T_0 = \frac{1}{2}T_{\max}\frac{\mathrm{Ca}_0^2}{\mathrm{Ca}_0^2 + \mathrm{ECa}_{50}^2}\left[1 - \cos\left(\frac{0.25}{m l_{\mathrm{R}}\sqrt{2\mathrm{E}_{11} + 1} + b} + 1\right)\pi\right] \quad (A5)$$

In *Eq. A5*, m and b are material constants, and ECa_{50} is the length-dependent calcium sensitivity given by

$$\mathrm{ECa}_{50} = \frac{(\mathrm{Ca}_0)_{\max}}{\sqrt{\exp\left[B\left(l_{\mathrm{R}}\sqrt{2\mathrm{E}_{11} + 1} - l_0\right)\right] - 1}} \quad (A6)$$

where B is a constant, $(\mathrm{Ca}_0)_{\max}$ is the maximum peak intracellular calcium concentration, l_0 is the sarcomere length at which no active tension develops, and l_{R} is the stress-free sarcomere length. Material constants for active contraction were taken to be (32) as follows: Ca_0 = 4.35 μmol/l, $(\mathrm{Ca}_0)_{\max}$ = 4.35 μmol/l, B = 4.75 $\mu\mathrm{m}^{-1}$, l_0 = 1.58 μm, m = 1.0489 s/μm, b = −1.429 s, and l_{R} = 1.85 μm. Based on biaxial stretching experiments, cross-fiber, in-plane active stress equivalent to 40% of that along the myocardial fiber direction was also added.

Determination of the patient-specific material parameter T_{max} is described in the main text.

ACKNOWLEDGMENTS

We thank Pamela Derish in the Department of Surgery at UCSF for proofing the manuscript.

GRANTS

This study was supported by National Heart, Lung, and Blood Institute Research Grants R01 HL-077921 and R01 HL-086400 (J. M Guccione); R01 HL-063348 and R01 HL-084431 (M. B. Ratcliffe); HL-084529 (G. S. Kassab); and the National Research Foundation, Singapore under its Cooperative Basic Research Grant administered by the Singapore Ministry of Health's National Medical Research council NMRC/EDG/2011 (L. Zhong). The support of these agencies is gratefully acknowledged.

DISCLOSURES

No conflicts of interest, financial or otherwise, are declared by the author(s).

AUTHOR CONTRIBUTIONS

Author contributions: L.C.L., J.F.W., J.L.N., G.S.K., and J.M.G. conception and design of research; L.C.L., J.F.W., L.Z., D.K., Z.Z., L.G., M.B.R., and E.H. analyzed data; L.C.L., G.S.K., and J.M.G. interpreted results of experiments; L.C.L. prepared figures; L.C.L. drafted manuscript; L.C.L., L.Z., D.K., T.I.Z., G.S.K., and J.M.G. edited and revised manuscript; E.H. performed experiments; J.M.G. approved final version of manuscript.

REFERENCES

1. **Aikawa Y, Rohde L, Plehn J, Greaves SC, Menapace F, Arnold MO, Rouleau JL, Pfeffer MA, Lee RT, Solomon SD.** Regional wall stress predicts ventricular remodeling after anteroseptal myocardial infarction in the Healing and Early Afterload Reducing Trial (HEART): an echocardiography-based structural analysis. *Am Heart J* 141: 234–242, 2001.
2. **Aroney CN, Herrmann HC, Semigran MJ, William G, Boucher CA, Fifer MA.** Linearity of the left ventricular end-systolic pressure volume relation in patients with severe heart failure. *J Am Coll Cardiol* 14: 127–134, 1989.
3. **Athanasuleas CL, Stanley AWH, Buckberg GD.** Restoration of contractile function in the enlarged left ventricle by exclusion of remodeled akinetic anterior segment: surgical strategy, myocardial protection and angiographic results. *J Card Surg* 13: 418–428, 1998.
4. **Athanasuleas CL, Buckberg GD, Stanley AWH, Siler W, Dor V, Donato MD, Menicanti L, Oliveria SA, Beyersdorf F, Kron IL, Suma H, Kouchoukos NT, Moore W, McCarthy PM, Oz MC, Fontan F, Scott ML, Accola KA; RESTORE group.** Surgical ventricular restoration in the treatment of congestive heart failure due to post-infarction ventricular dilation. *J Am Coll Cardiol* 44: 1439–1445, 2004.
5. **Bourlag BA, Lam CSP, Roger VL, Rodeheffer RJ, Redfield MM.** Contractility and ventricular systolic stiffening in hypertensive heart disease: insights into the pathogenesis of heart failure with preserved ejection fraction. *J Am Coll Cardiol* 54: 410–418, 2009.
6. **Brinke EA, Klautz RJ, Tulner SA, Verwey HF, Bax JJ, Schalij MJ, van der Wall EE, Versteegh MI, Dion RA, Steendijk P.** Long-term effects of surgical ventricular restoration with additional restrictive mitral annuloplasty and/or coronary artery bypass grafting on left ventricular function: Six-month follow-up by pressure-volume loops. *J Thorac Cardiovasc Surg* 140: 1338–1334, 2010.
7. **Buckberg G, Athanasuleas C, Conte J.** Surgical ventricular restoration for the treatment of heart failure. *Nat Rev Cardiol* 9: 703–716, 2012.
8. **Buckberg GD, Athanasuleas CL, Wechsler AS, Beyersdorf F, Conte JV, Strobeck JE.** The STICH trial unraveled. *Eur J Heart Fail* 12: 1024–1027, 2010.
9. **Choi HF, D'Hooge J, Rademakers FE, Claus P.** Influence of left ventricular shape on passive filling properties and end-diastolic fiber stress and strain. *J Biomech* 43: 1745–1753, 2010.
10. **Dang AB, Guccione JM, Zhang P, Wallace AW, Gorman RC, Gorman JH 3rd, Ratcliffe MB.** Effect of ventricular size and patch stiffness in surgical anterior ventricular restoration: a finite element model study. *Ann Thorac Surg* 79: 185–193, 2005.
11. **Dang AB, Guccione JM, Mishell JM, Zhang P, Wallace AW, Gorman RC, Gorman JH 3rd, Ratcliffe MB.** Akinetic myocardial infarcts must contain contracting myocytes: finite-element model study. *Am J Physiol Heart Circ Physiol* 288: H1844–H1850, 2005.
12. **Donato MD, Sabatier M, Dor V, Gensini GF, Toso A, Maioli M, Stanley AWH, Athanasuleas C, Buckberg G.** Effects of the DOR procedure on left ventricular dimension and shape and geometric correlates of mitral regurgitation one year after surgery. *J Thorac Cardiovasc Surg* 121: 91–96, 2001.
13. **Donato MD, Fantini F, Toso A, Castelvecchio S, Menicanti L, Annest L, Burkhoff D.** Impact of surgical ventricular reconstruction on stroke volume in patients with ischemic cardiomyopathy. *J Thorac Cardiovasc Surg* 140: 1325–1331, 2010.
14. **Geerts L, Kerckhoffs R, Bovendeerd P, Arts T.** Towards patient specific models of cardiac mechanics: a sensitivity study. In: *Lecture Notes in Computer Science-Functional Imaging and Modeling of the Heart, Proceedings.* Berlin: Springer-Verlag 81–90, 2003.
15. **Grossman W.** Cardiac hypertrophy: useful adaptation or pathologic process? *Am J Med* 69: 576–584, 1980.
16. **Guccione JM, Moonly SM, Wallace AW, Ratcliffe MB.** Residual stress produced by ventricular volume reduction surgery has little effect on ventricular function and mechanics: a finite element model study. *J Thorac Cardiovasc Surg* 122: 592–599, 2001.
17. **Guccione JM, Waldman LK, McCulloch AD.** Mechanics of active contraction in cardiac muscle. II. Cylindrical models of the systolic left ventricle. *J Biomech Eng* 115: 82–90, 1993.
18. **Guccione JM, Costa KD, McCulloch AD.** Finite element stress analysis of left ventricular mechanics in the beating dog heart. *J Biomech* 28: 1167–1177, 1995.
19. **Isomura T, Hoshino J, Fukada Y, Kitamura A, Katahira S, Kondo T, Iwasaki T, Buckberg G; RESTORE Group.** Volume reduction rate by surgical ventricular restoration determines late outcome in ischemic cardiomyopathy. *Eur J Heart Fail* 13: 423–431, 2011.
20. **Isomura T, Horii T, Suma H, Buckberg GD; RESTORE Group.** Septal anterior ventricular exclusion (Pacopexy) for ischemic dilated cardiomyopathy: treat form not disease. *Eur J Cardiothorac Surg* 29, *Suppl* 1: S245–S250, 2006.
21. **Jones RH, Velazquez EJ, Michler RE, Sopko G, Oh JK, O'Connor CM, Hill JA, Menicanti L, Sadowski Z, Desvigne-Nickens P, Rouleau JL, Lee KL; STICH Hypothesis 2 Investigators.** Coronary bypass surgery with or without surgical ventricular reconstruction. *N Engl J Med* 360: 1705–1717, 2009.
22. **Menicanti L, Castelvecchio S, Ranucci M, Frigiola A, Santambrogio C, Vincentiis C, Brankovic J, Donato MD.** Surgical therapy for ischemic heart failure: single-center experience with surgical anterior ventricular restoration. *J Thorac Cardiovasc Surg* 134: 433–441, 2007.
23. **Menicanti L, Donato MD.** The Dor procedure: What has changed after fifteen years of clinical practice? *J Thorac Cardiovasc Surg* 124: 886–890, 2002.
24. **Prucz RB, Weiss ES, Patel ND, Nwakanma LU, Baumgartner WA, Conte JV.** Coronary artery bypass grafting with or without surgical ventricular restoration: a comparison. *Ann Thorac Surg* 86: 806–814, 2008.
25. **Retzlaff B, Voss B, Albrecht W, Lange R, Hinson AG, Sabbah HN, Lee RJ, Bauenrschmitt R.** First in man experience with left ventricular reconstruction in patients with systolic heart failure using a novel approach of biopolymer hydrogel implantation (Abstract). *Circulation* 122: A19753, 2010.
26. **Rouleau JL, Michler RE, Velazquez EJ, Oh JK, O'Conner CM, Desvigne-Nickens P, Sopko G, Lee KL, Jones RH.** The STICH trial: evidence-based conclusions. *Eur J Heart Fail* 12: 1028–1030, 2010.
27. **Salati M, Pajè A, Biasi PD, Fundaró P, Cialfi A, Santoli C.** Severe diastolic dysfunction after endoventriculoplasty. *J Thorac Cardiovasc Surg* 109: 694–701, 1995.
28. **Skelly NW, Allen JG, Arnaoutakis GJ, Weiss ES, Patel ND, Conte JV.** The impact of volume reduction on early and long-term outcomes in surgical ventricular restoration for severe heart failure. *Ann Thorac Surg* 91: 104–111, 2011.
29. **Strauer BE, Beer K, Heitlinger K, Höfling B.** Left ventricular systolic wall stress as a primary determinant of myocardial oxygen consumption: comparative studies in patients with normal left ventricular function, with pressure and volume overload and coronary heart disease. *Basic Res Cardiol* 72: 306–313, 1977.
30. **Streeter DD Jr, Spotnitz HM, Patel DP, Ross J Jr, Sonnenblick EH.** Fiber orientation in the canine left ventricle during diastole and systole. *Circ Res* 24: 339–347, 1969.

31. **Suga H, Sagawa K, Shoukas AA.** Load independence of the instantaneous pressure-volume ratio of the canine left ventricle and effects of epinephrine and heart rate on the ratio. *Circ Res* 32: 314–322, 1973.
32. **Sun K, Stander N, Jhun CS, Zhang Z, Suzuki T, Wang GY, Saeed M, Wallace AW, Tseng EE, Baker AJ, Saloner D, Einstein DR, Ratcliffe MB, Guccione JM.** A computationally efficient formal optimization of regional myocardial contractility in a sheep with left ventricular aneurysm. *J Biomech Eng* 131: 111001–1-111001–10, 2009.
33. **Sutton MG, Sharpe N.** Left ventricular remodeling after myocardial infarction: pathophysiology and therapy. *Circulation* 101: 2981–2988, 2000.
34. **Tulner SAF, Steendijk P, Klautz RJM, Bax JJ, Schalij MJ, van der Wall EE, Dion RAE.** Surgical ventricular restoration in patients with ischemic dilated cardiomyopathy: evaluation of systolic and diastolic ventricular function, wall stress, dyssynchrony, and mechanical efficiency by pressure-volume loops. *J Thorac Cardiovasc Surg* 132: 610–620, 2006.
35. **Velazquez EJ, Lee KL, O'Connor CM, Oh JK, Bonow RO, Pohost GM, Feldman AM, Mark DB, Panza JA, Sopko G.** The rationale and design of the surgical treatment for ischemic heart failure (STICH) trial. *J Thorac Cardiovasc Surg* 134: 1540–1547, 2007.
36. **Walker JC, Ratcliffe MB, Zhang P, Wallace AW, Fata B, Hsu EW, Saloner D, Guccione JM.** MRI based finite element analysis of left ventricular aneursym. *Am J Physiol Heart Circ Physiol* 289: H692–H700, 2005.
37. **Wijns W, Kolh P, Danchin N, Di Mario C, Falk V, Folliguet T, Garg S, Huber K, James S, Knuuti J.** Guidelines on myocardial revascularization. *Eur Heart J* 31: 2501–2555, 2010.
38. **Yin FC.** Ventricular wall stress. *Circ Res* 49: 829–842, 1982.
39. **Zhong L, Sola S, Tan RS, Le TT, Ghista DN, Kurra K, Navia JL, Kassab GS.** Effects of surgical ventricular restoration on left ventricular contractility assessed by a novel contractility index in patients with ischemic cardiomyopathy. *Am J Cardiol* 103: 674–679, 2009.
40. **Zhong L, Su Y, Gobeawan L, Sola S, Tan RS, Navia JL, Ghista DN, Chua T, Guccione JM, Kassab GS.** Impact of surgical ventricular restoration on ventricular shape, wall stress, and function in heart failure patients. *Am J Physiol Heart Circ Physiol* 300: H1653–H1660, 2011.